Aeroelastic behavior of launcher thermal insulation panel, accounting for various aerodynamic and structural models

L. Succi,* E. Carrera†
E. Zappino,‡ M. Cinefra§
Politecnico di Torino, Corso Duca degli Abruzzi 24, 10129 Torino, Italy.

Versatile Thermal Insulation panels, have been introduced for the first time with U.S. space launchers during the '60, and immediately represented an element of high complexity, due the wide range of design parameters and the difficult operating conditions. Cases of flutter affecting VTI panels, have been observed since the first applications, stimulating the development of theories able to predict the phenomenon with sufficient accuracy. Numerical study of the panel flutter, has led to the development of different structural and aerodynamic models, useful for investigate this aeroelastic stability. The quasi-steady Piston Theory formulation may be applied only above $M = 1.5$, reducing the study capability to the supersonic range. This work proposes an un-steady formulation of the Piston Theory, derived by Vedeneev, aiming to extend its range of validity also for $1.3 < M < 1.5$. Various comparison between these aerodynamic theories, have been carried out in order to underline the main differences in the previous range of Mach and in the accuracy with which the critical conditions are detected. Hand in hand, have been tested different structural models, of increasing complexity, based on $1D$ and $2D$ formulation, and also panels with a more advanced structure, multi-layer and sandwich and for last, a typical VTI configuration consists of a semi-circle sandwich panel. Using Shell models such as Equivalent Single Layer or Layer Wise, you may observe relevant variations in final results, highlighting the necessity of more complex structural models in Multi-Layered panels.

Nomenclature

$\boldsymbol{u}$	Displacement vector
u_x, u_y, u_z	Displacement components in the x, y and z directions
x, y, z	Coordinates reference system
$\boldsymbol{\sigma}$	Stress vector
$\boldsymbol{\epsilon}$	Strain vector
$\boldsymbol{D}$	Linear differential operator matrix
$\boldsymbol{C}$	Material stiffness matrix
F_τ	Cross-section function
$\boldsymbol{u}_\tau$	Generalized displacement vector
N	Order of the expansion above the cross-section for the TE models
$\boldsymbol{q}_{\tau i}$	Nodal displacement vector
N_i	Shape function

*Student, Department of Mechanical and Aerospace Engineering, lorenzo.succi@polito.it
†Professor, Department of Mechanical and Aerospace Engineering, erasmo.carrera@polito.it, AIAA Member
‡Ph.D. Student, Department of Mechanical and Aerospace Engineering, enrico.zappino@polito.it
§Ph.D. Research Assistant, Department of Mechanical and Aerospace Engineering, maria.cinefra@polito.it

δ	Virtual variation
L_{int}	Internal work
L_{ext}	External work
L_{ine}	Work of the inertial loadings
$\boldsymbol{E}$	Young module
$\boldsymbol{G}$	Shear module
ρ	Flow density
ρ_m	Panel material density
μ	ρ on ρ_m ratio
$\boldsymbol{a}$	speed of sound
$\boldsymbol{h}$	panel thickness
$\boldsymbol{w}$	panel vertical displacement
$\boldsymbol{h}$	panel thickness
$\boldsymbol{d}$	panel width
$\boldsymbol{M}$	Mach number
$\boldsymbol{h}$	panel thickness
ω	frequency
$\boldsymbol{W}$	harmonic displacement law amplitude
$\bar{L}$	non-dimensional panel length
$\boldsymbol{L}$	dimensional panel length
γ	heat capacity ratio
$\boldsymbol{R}$	specific gas constant
$\boldsymbol{T}$	Flow temperature
$\boldsymbol{V}$	Flow relative speed

I. Introduction

The first cases of panel flutter on space launchers, were observed in the '60 during Saturn V, Atlas-Centaur and Titan development(NASA 1965).[1] In spite flutter of wing surfaces, panel flutter is commonly known as a non-destructive instability, whose oscillations tend to a cycle of limited amplitude. This significant feature is determined by the presence of structural non-linearities, produced during the flexional motion of high amplitude.[2] Nevertheless, panels subjected to this instability, can fail realistically due to fatigue stress. Hence, a successful panel design should include both reliability during the critical phase of the flight and low structural mass. The European Space Agency has been involved for years in the Future Launcher Preparatory Program FLPP, within which take place a specific program dedicated to the set of technologies, useful to improve the cryogenic upper stage design CUST.[3] In particular, has been proposed to use Versatile Thermal Insulation VTI panels to protect the cryogenic tanks of the upper stage, during the most stressful missione phase in terms of thermal and structural stress; successively this panels are released using pyrotechnic charges. This phase can last for about 80s, during which the launcher starts from Mach 0 and became supersonic. The thermal insulation function of the panel is mandatory to ensure the necessary protection of the cryogenic stage, above all during the transonic segment. Usually in this phase, the panels encounter an high kinetic heating due to the combined effects of speed, shocks and high air density. The panel is also subjected to a considerable thermal gradient between the outer surface and the inner. Aiming to ensure a cryogenic temperature in the internal cavity of the upper stage, a cooling system based on liquid nitrogen, is interposed between the tanks and the panel structure. On the basis of this premise, you get a context of high complexity within which three entities interact each other. These are represented by the aerodynamic, the structural features, and the thermal field. Their interaction define an aerothermoelastic problem. The large number of variables in VTI panel design, make the flutter analysis almost unique. Actually, there are very few documents in literature concerning flutter of VTI panels, so both experimental and numerical investigation should be useful for a better understanding of panels behavior. This paper is intended to continue the research carried out by Polytechnic of Turin, concerning VTI design and flutter analysis, introducing a un-steady formulation of the piston theory, developed by Vedeneev (2012), to accompany and eventually refine, the quasi-steady formulation(Ashley - Zartarian , 1956)[4] results. Aim of this improved aerodynamic theory, is to extend panel flutter analysis to the low supersonic regime, in order to numerically predict the single mode flutter, if present, and to enhance the accuracy in flutter boundary definition for the same regime. This recent reformulation of the historically known q-s Piston Theory, has been used with different structural model developed within the Carrera Unified Formulation CUF, in particular an advanced Shell Model.[5] Through it, has been tested different panels geometry, internal structure and boundary conditions.

II. The Aeroelastic Model

The aeroelastic model used in the present work can be expressed in terms of equilibrium of the works virtual variations. From the Principle of Virtual Displacement (PVD) it is possible to write:

$$\delta L_{int} + \delta L_{ine} = \delta L_a \tag{1}$$

where L_{int} is the work due to the elastic forces, L_{ine} is the inertial work and L_a is the work made by the aerodynamic forces. δ denotes the virtual variation. The formulation of these contributes will be detailed in the following sections.

The whole theoretical model refers to the following notation. The transposed displacement vector is defined as

$$\mathbf{u}(x, y, z) = \left\{ \begin{array}{ccc} u_x & u_y & u_z \end{array} \right\}^T \tag{2}$$

where x, y, and z are orthonormal axes.

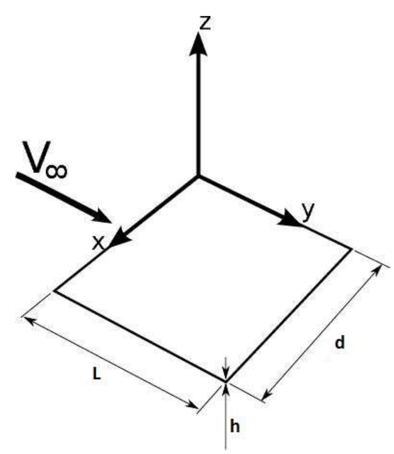

Figure 1. Reference system.

A. Structural Model

Stress, $\boldsymbol{\sigma}$, and strain, $\boldsymbol{\epsilon}$, components are grouped as follows:

$$\boldsymbol{\sigma}_p = \left\{ \begin{array}{cccccc} \sigma_{xx} & \sigma_{yy} & \sigma_{zz} & \sigma_{xy} & \sigma_{xz} & \sigma_{yz} \end{array} \right\}^T, \boldsymbol{\epsilon}_p = \left\{ \begin{array}{cccccc} \epsilon_{xx} & \epsilon_{yy} & \epsilon_{zz} & \epsilon_{xy} & \epsilon_{xz} & \epsilon_{yz} \end{array} \right\}^T \tag{3}$$

Linear strain-displacement relations are used,

$$\boldsymbol{\epsilon} = \boldsymbol{D}\mathbf{u} \tag{4}$$

Where

$$\boldsymbol{D} = \begin{bmatrix} \frac{\partial}{\partial x} & 0 & 0 \\ 0 & \frac{\partial}{\partial y} & 0 \\ 0 & 0 & \frac{\partial}{\partial z} \\ \frac{\partial}{\partial y} & \frac{\partial}{\partial x} & 0 \\ \frac{\partial}{\partial z} & 0 & \frac{\partial}{\partial x} \\ 0 & \frac{\partial}{\partial z} & \frac{\partial}{\partial y} \end{bmatrix} \tag{5}$$

Constitutive laws are exploited to obtain stress components,

$$\boldsymbol{\sigma} = \boldsymbol{C}\boldsymbol{\epsilon} \tag{6}$$

The components of $\boldsymbol{C}$ are the material coefficients whose explicit expressions are not reported here for the sake of brevity, they can be found in.[6]

1. *Displacement models and Finite Element Formulation*

The generic three dimensional displacements model can be written as follow:

$$\mathbf{u}(x,y,z) = f(x,y,z;t) \tag{7}$$

The three dimensional formulation can be reduced to the two- and one-dimensional formulation by introducing the function f_τ. This function introduce an expansion in the thickens of the structure (2D formulation) or in the cross-section (1D formulation).

$$\begin{aligned} 2D &\longrightarrow u(x,y,z) = f(x,y;t)F_\tau^{2D}(z), \qquad \tau = 1,2,....,N \\ 1D &\longrightarrow u(x,y,z) = f(y;t)F_\tau^{1D}(x,z), \qquad \tau = 1,2,....,N \end{aligned} \tag{8}$$

In the formulation of F_τ^{2D} and F_τ^{1D} can be used different polynomials. A complete overview of the function used in the 1D formulation can be found in the book by Carrea *et al.*[7] In this work two different expansion are used. The first one based on the Taylor formulation[8] (TE), the second one based on the Lagrange formulation[9] were the unknowns are the displacements only. The formulation of the 2D expansion[10] can be derived with a Equivalent Single Layer (ESL) approach or in a Layer Wise (LW) formulation. In this work the second approach, layer wise formulation, is used.

The model derived by the introduction of the F_τ^{n-D} can be solved by using different approaches. In this work the FEM approach is used. By introducing the shape functions, N_i, the eq.8 can be written in the following formulation:

$$\begin{aligned} 2D &\longrightarrow u(x,y,z) = q_{i\tau}(t)N_i(x,y)F_\tau^{2D}(z), \qquad i = 1,2,....,K \\ 1D &\longrightarrow u(x,y,z) = q_{i\tau}(t)N_i(y)F_\tau^{1D}(x,z), \qquad i = 1,2,....,K \end{aligned} \tag{9}$$

Where the function N_i are the Lagrange function and K is the number of node of the element used.

2. *Stiffness Matrix*

The stiffness and mass matrices can be derived in the frameworks of the CUF formulation introduced by Carrera[11] that allow to derive a unified formulation where K and N can be considered as an input of the problem.

The virtual variation of the strain energy is given by:

$$\begin{aligned} \delta L_{int} &= \int_V (\delta \boldsymbol{\epsilon}^T \boldsymbol{\sigma}) dV = \\ &= \int_V \delta \mathbf{q}_{js}^T \Big[\boldsymbol{D}^T \Big(N_j F_s \boldsymbol{I}\Big)\Big] \boldsymbol{C} \Big[\boldsymbol{D}\Big(N_i F_\tau \boldsymbol{I}\Big)\Big] \mathbf{q}_{\tau i} dV \end{aligned} \tag{10}$$

The variation of the internal work is then written by means of the CUF fundamental nucleus $\mathbf{K}^{ij\tau s}$:

$$\delta L_{int} = \delta \mathbf{q}_{js}^T \mathbf{K}^{ij\tau s} \mathbf{q}_{\tau i} \tag{11}$$

The fundamental nucleus is a 3×3 matrix with a fixed formulation. The explicit forms of the 9 components of $\mathbf{K}^{ij\tau s}$ are not reported here, they can be found in literature.[12]

3. Mass Matrix

The mass matrix can be derived in the same way by considering the inertial energy expressed by:

$$\delta L_{ine} = \int_V (\rho \ddot{\boldsymbol{u}} \delta \boldsymbol{u}^T) dV \tag{12}$$

where ρ stands for the density of the material, and $\ddot{\boldsymbol{u}}$ is the acceleration vector. Eq. 12 is rewritten using Eq.s 4:

$$\delta L_{ine} = \int_V \delta \boldsymbol{q}_{js}^T N_i \rho (F_s \boldsymbol{I})(F_\tau \boldsymbol{I}) N_j \ddot{\boldsymbol{q}}_{i\tau} dV \tag{13}$$

where $\ddot{\boldsymbol{q}}$ is the nodal acceleration vector. The last equation can be rewritten in the following compact manner:

$$\delta L_{ine} = \delta \boldsymbol{q}_{sj}^T \boldsymbol{M}^{ij\tau s} \ddot{\boldsymbol{q}}_{\tau i} \tag{14}$$

where $\boldsymbol{M}^{ij\tau s}$ is the mass matrix in the form of the fundamental nucleus. No assumptions on the approximation order have been done to obtain the fundamental nucleus. It is therefore possible to obtain refined 1D models without changing the formal expression of the nucleus components. This is the key-point of CUF which permits, with only nine FORTRAN statements, to implement any-order one-dimensional theories.

B. Aerodynamic model

There are relevant advantages to using the Piston Theory in the quasi-steady formulation. Compared to theories such as potential flow theory or numerical methods based on DNS scheme, Piston Theory results easier to implement and solve. However, its more simplistic approach costs in terms of accuracy, but only outside its range of applicability. The vast literature available, has shown how this theory is valid starting from Mach 1.5 and correctly predicts occurrences of coupled mode flutter. During the last years, Vedeneev has proposed an un-steady formulation of the Piston Theory, obtained from the potential flow theory. This formulation aims to extends its use also to lower Mach numbers, below previous limit, and attempts to notice single-mode flutter occurrence. This instability phenomenon, is also called high-frequency flutter and unlike the coupled-mode flutter, it involves only one degree of freedom, not requiring modes coalescence. The high-frequency feature suggests that panels with higher stiffness and only one dimension, the thickness, negligible, are more subjected to this instability. In fact, the vast literature concerning panel flutter, shown how coupled-mode flutter affects mainly thin structures, with the longest side in the same flow direction. Few paper are actually devoted to single-mode flutter study using more complex aerodynamic theories. First researches date back to 40' and 60' (Bolotin,[13] 1963; Garric and Rubinow,[14] 1946; Miles,[15] 1959; Nelson and Cunningham,[16] 1956; Dowell, 1967,[17] 1971,[18] 1974[19]), were taken more recently by Gordier and Visbal[20] (2002), Vedeneev (2012), Hashimoto[21] (2009). In its theoretical studies on limit cycle amplitude, Vedeneev notified how much rapid was the amplitude increase while entering single-mode flutter region, compared to coupled-mode flutter occurrence. Moreover, has been postulated how flutter boundaries are not influenced by gas density (in contrast with coupled-mode) and also how the instability could occur in several eigenmodes at same time. Piston theory has been obtained starting from the un-steady gas pressure expression of the potential flow theory:[22]

$$p(W,\omega t) = \frac{\mu M}{\sqrt{M^2-1}}\Bigg(-i\omega W(x) + M\frac{dW(x)}{dy} + \frac{\mu\omega}{(M^2-1)^{\frac{3}{2}}} \int_0^x (-i\omega W(\xi) + M\frac{dW(\xi}{d\xi})xe^{(}\frac{iM\omega(x-\xi}{M^2-1})(iJ_0(\frac{-\omega(x-\xi)}{M^2-1})+ MJ_1(\frac{-\omega(x-\xi)}{M^2-1})\Bigg)\,d\xi \tag{15}$$

This expression shown the vertical displacement law of the panel, considering it as harmonic:

$$w(y,t) = W(y)e^{-i\omega t} \tag{16}$$

Omitting integral terms in 15, unsteady Piston theory can be obtained:

$$p(W,\omega) = \frac{\mu M}{\sqrt{M^2-1}}\left(-i\omega W(y) + M\frac{\partial W(y)}{\partial y}\right) \tag{17}$$

As well as the quasi-steady Piston Theory, the two principal differences reside in the transition from temporal domain to the frequencies domain, and the introduction of a complex term. As is known theoretically, the imaginary element is associated to a damping function, in this case the aerodynamic damping, represented by $W(y)$. Instead, the other block, who multiply $\frac{\partial W(y)}{\partial y}$, represent the aerodynamic stiffness. Previous Piston Theory has been written in dimensionless form, however our application requested a conversion in dimensional form, rewritten as follows:

$$p(W,\omega) = \frac{a\rho_m\mu M}{\sqrt{M^2-1}}\left(-i\omega h W(y) + aM\frac{\partial W(y)}{\partial y}\right) \tag{18}$$

In order to represent also single-mode flutter, you could provide a fractionary term that becomes negative for $M < \sqrt{2}$. It is also found in quasi-steady Piston Theory formulation, and plays the role of a correction term for the low supersonic range. Here the following representation:

$$p(W,\omega) = \frac{a\rho_m\mu M}{\sqrt{M^2-1}}\left(-i\omega h\frac{M^2-2}{M^2-1}W(y) + aM\frac{\partial W(y)}{\partial y}\right) \tag{19}$$

If the first formulation is better for coupled-mode flutter analysis, the second is more indicated for single-mode instability, because for $M < \sqrt{2}$, always predict this flutter type. Results collected by these two formulation, have been compared with those provided by quasi-steady Piston theory. A large amount of publications were focused on aeroelastic application using Piston Theory, it provided results in good agree with experimental tests, but only above $M = 1.5$. This formulation is written below:

$$p(y,t) = \frac{\rho V}{\sqrt{M^2-1}}\left(\frac{M^2-2}{M^2-1}\frac{\partial w}{\partial t} + V\frac{\partial w}{\partial y}\right) \tag{20}$$

1. *Aerodynamic matrices*

The implementation of the aerodynamic model within the FE formulation, was made by applying the principle of virtual work. Considering the pressure field Δp acting on the infinitesime element $\partial\Lambda$ of the panel of generic length Λ, you can write:

$$\delta L_{\delta u}^{\Delta p} = \int_\Lambda (\delta u \Delta p)\,d\Lambda \tag{21}$$

Substituting the Piston Theory expression to Δp, and the displacement field from the CUF formulation in δu, you can obtain the Aerodynamic stiffness matrix and the Aerodynamic damping matrix. Following matrix are for $1D$ Beam structural model. This representation may be extended also for $2D$ Shell model, only replacing the integration field respectively of the shape functions, now dependent by variables x and y that lie on the component's surface , and of the CUF functions, dependent by the variable z along the thickness.

$$[K_a^{ij\tau s}] = \frac{a^2 \rho_m \mu M^2}{\sqrt{M_\infty^2 - 1}} \int_x (F_\tau F_s)\, dx \begin{bmatrix} 0 & 0 & 0 \\ 0 & \int_L N_i \frac{\partial N_j}{\partial y}\, dy & 0 \\ 0 & 0 & 0 \end{bmatrix}$$

$$[D_a^{ij\tau s}] = \frac{-i\omega \rho_m a \mu M h}{\sqrt{M_\infty^2 - 1}} \int_x (F_\tau F_s)\, dx \begin{bmatrix} 0 & 0 & 0 \\ 0 & \int_L N_i N_j\, dy & 0 \\ 0 & 0 & 0 \end{bmatrix}$$

III. Results

A. Aeroelastic model validation

In order to validate the aerodynamic theory, has been chosen a test case provided by Vedeneev consist of a 2D plate model, of aspect ratio $\bar{L} = 250$, simply supported on both the edges, mounted into an infinite absolutely rigid plane, with the gas flow that occupies the upper half-plane, while in the lower half-plane constant undisturbed gas flow pressure is imposed. As analysis parameters have been chosen $\rho_m = 7500$ Kg/m^3, $\rho = 0.91$ Kg/m^3, $a = 328.6$ m/s. The panel has infinite dimension along the orthogonal direction to the flow. Its critical conditions are calculated not by Finite Elements methods, but through iterative methods based on Galerkin algorithm. Structural model used by Polito is based on the Carrera Unified Formulation CUF, and consist of a 1D FSDT model based on 10 Beam elements, with 4 dof for each and 684 global dof. A low-order method has been used to better approximate the two-dimensional model of Vedeneev. Models of higher order would have introduced modal contents related the neglected dimension. Panel geometry is $h = 0.002$ m, $L = 0.5$ m, $d = 1$ m. The first four eigenvalues has been calculated in correspondence of $M = 1.6, M = 1.05$ and in vacuum condition. Assuming an evaluation error of the 2D

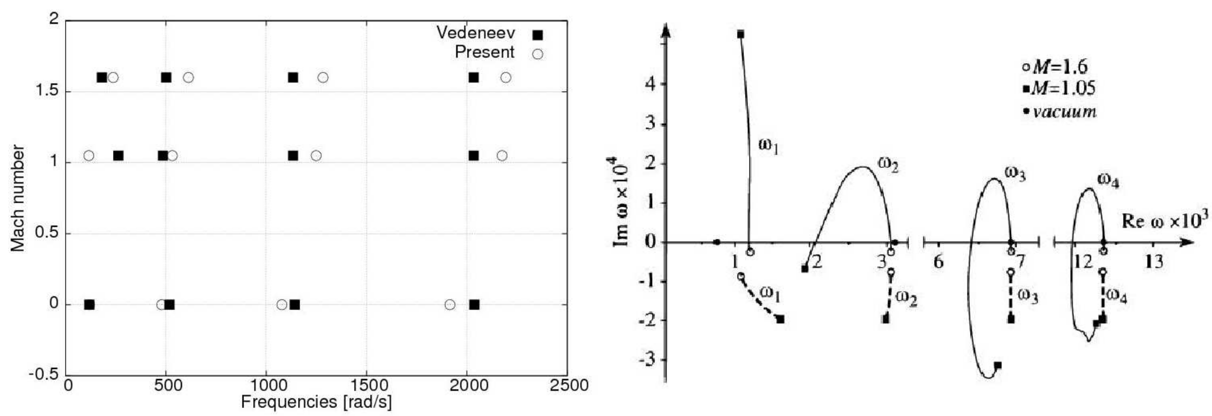

Figure 2. First four eigenfrequencies obtained with 18 Piston Theory (sx); eigenfrequencies obtained through Potential flow theory,[23] continuous curves, and Piston theory, dashed curves, (dx)

plate's frequencies, of which there aren't explicit values, results obtained by FSDT model show to be in good agree with the test case. The following table, shows numerical values obtained. Test case frequencies have been rewritten in dimensional form through a/h multiplier.

$$\bar{\omega} = \frac{\omega}{a/h} \tag{22}$$

Results obtained by Vedeneev, were in sufficient agree with those of Polito, in particular for higher modes. The lack of numerical data concerning the 2D plate, introduced an evaluation error hard to estimate correctly, but at least of $\pm 10\%$ on the referring value. At $M = 1.6$, un-steady formulation shows to be in good agree with Potential flow theory results, but at the same time it is totally inadequate for $M = 1.05$. At this Mach number, Piston theory doesn't show stability transition of the first eigenmode, but rather each eigenmodes become more stable. These results suggest the total inaccuracy of Piston Theory for very low

Table 1. Eigenfrequencies obtained respectively with 2D plate theory and FSDT model

	plate Vedeneev			FSDT present model		
			$[rad/s]$			
$Mode$	$Vacuum$	$M = 1.05$	$M = 1.6$	$Vacuum$	$M = 1.05$	$M = 1.6$
1	118.3	262.9	180.7	119.8	115.4	236.6
2	517.5	484.7	501.1	479.0	531.8	612.3
3	1141.9	1133.7	1133.7	1077.7	1248.6	1282.9
4	2037.3	2034.0	2034.0	1915.6	2175.2	2194.2

supersonic range. Instead, Potential flow theory, is able to predict single-mode flutter of the first mode at $M = 1.05$.

B. Comparison of different aerodynamic and structural models

In order to obtain more detailed results, un-steady Piston theory has been used associated with different structural models. The new test case is characterized by the following parameters: $E = 75 \times 10^9\ Pa$, $G = 28 \times 10^9\ Pa$, $\nu = 0.3$, $\rho_m = 2700\ Kg/m^3$, $L = 0.5\ m$, $d = 1\ m$, $T = 228\ K$, $\gamma = 1.4$, $R = 287\ J/KgK$, $a = 302.7\ m/s$, $\rho = 0.363\ Kg/m^3$.

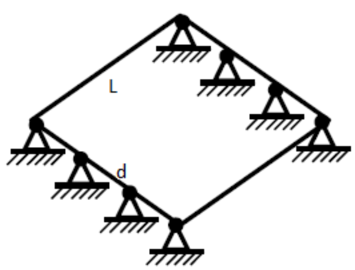

Figure 3. Test case panel

The panel is simply supported on two opposite sides. The short sides are aligned with the flow direction. The comparison among different models, was made on the identification of panel's critical conditions, focusing on the first critical mach and the corresponding flutter frequency. Tests already performed on the same configuration but using quasi-steady Piston Theory formulation, has been adopted as referring values for the second validation step. As previously mentioned, different structural models have been used. These models are both based on the CUF, but are divided in 1D Beam-based models, and 2D Shell models. For the first class, have been used high-order methods as well as EDTN 2-3-4, while for the second class have been used Layer-Wise LW models of order 2-3-4 and Equivalent Single Layer ESL of the same orders. Below, two tables show models information and results obtained:

Table 2. Critical Mach and flutter frequencies with different structural and aerodynamic models

		Critical Mach			Flutter frequencies [Hz]			
	Model	$q-sPT$ 20	$u-sPT$ 18	$u-sPT$ 19	$q-sPT$ 20	$u-sPT$ 18	$u-sPT$ 19	*NDOF*
	*EDTN*2	4.344	4.333	4.333	65.276	66.651	71.459	558
1*D*	*EDTN*3	4.806	4.795	4.794	69.566	71.027	77.075	930
	*EDTN*4	4.326	4.313	4.313	65.092	66.463	71.220	1395
	*LW*2	5.220	5.209	5.208	71.099	72.559	79.602	726
	*LW*3	4.347	4.336	4.336	65.168	66.537	71.340	1089
2*D*	*LW*4	4.347	4.336	4.336	66.517	66.537	71.340	1452
	*ESL*2	4.351	4.340	4.340	65.208	66.587	71.400	726
	*ESL*3	4.350	4.339	4.339	65.191	66.568	71.379	1089
	*ESL*4	4.349	4.338	4.338	65.185	66.559	71.371	1452

C. Low supersonic range analysis

The second comparison made, aims to point out the panel behavior for flow density progressively higher in terms of growth of critical conditions, both of coupled mode flutter and single mode flutter. Comparing the un-steady and the quasi-steady Piston Theory formulation each other, it was possible to validates the first of these in the supersonic range $M > 1.5$, and at same time, provides a new set of information for Mach numbers just below $M = 1.5$. Vedeneev test case shown how the un-steady formulation was still unreliable for very low supersonic regime, hence this study focuses the attention on a more restricted range, $1.25 < M < 1.5$. Within it, has been observed different modes behavior, furthermore the increase of density causes the advance of coupled mode flutter occurrences, until the modes who coalesce become one unstable ad the other stable, already starting from the lower mach. Densities used for the tests are $\rho_1 = 0.363$ $\rho_2 = 0.5$ $\rho_3 = 0.8$ $\rho_4 = 0.86$ $\rho_5 = 0.9$ $\rho_6 = 1.0$ $[Kg/m^3]$. Aerodynamic models used refer to equation 19 and 20, while the structural model chosen is a Layer wise of the forth order, characterized by 1452 dof. Results provides by un-steady formulation could be interpreted stating that modes having negative or almost null damp, are stable. Un-steady formulation highlights in the range $1.25 < M < 1.5$ a different stability field, theoretically less conservative than what happens with 20, that suggests experimental tests to investigate this trend. Increasing the flow density are observed two main effects: modes previously involved in the coalescence phenomenon, typical of coupled-mode flutter, now separate in two distinct modes one of which is always stable and the other unstable, furthermore damping absolute value become even more high. Following results are related to previous flow density:

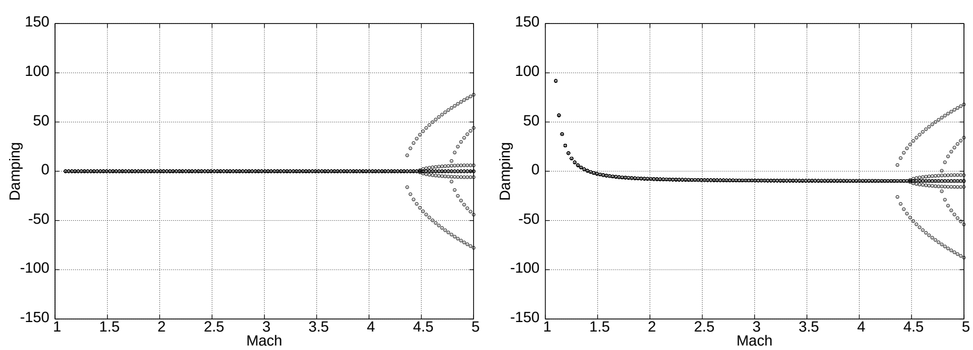

(a) Modal damping with un-steady PT 19

(b) Modal damping with q-steady PT 20

Figure 4. Modal damping trend with different aerodynamic models with $\rho = 0.363$ $[Kg/m^3]$ highlighting main differences in low supersonic range

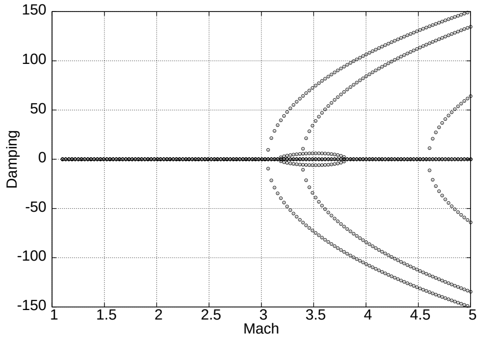

(a) Modal damping with un-steady PT 19

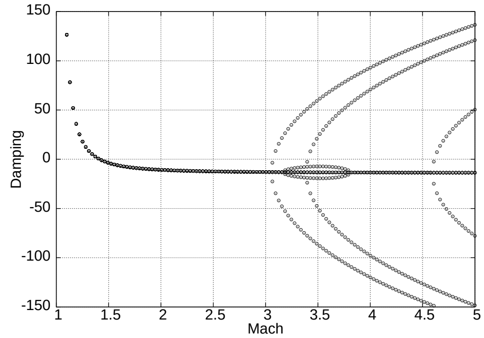

(b) Modal damping with q-steady PT 20

Figure 5. Modal damping trend with $\rho = 0.5$ $[Kg/m^3]$

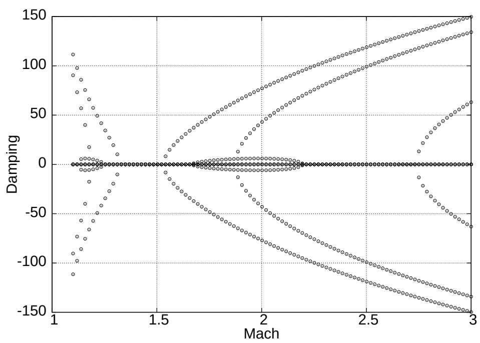

(a) Modal damping with un-steady PT 19

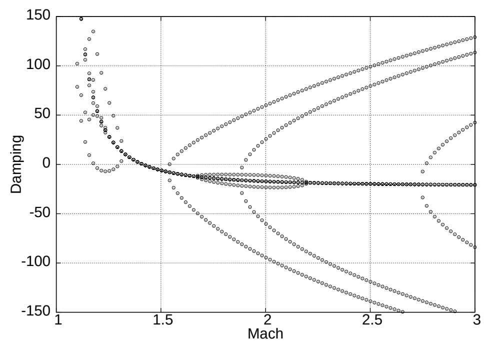

(b) Modal damping with q-steady PT 20

Figure 6. Modal damping trend with $\rho = 0.8$ $[Kg/m^3]$

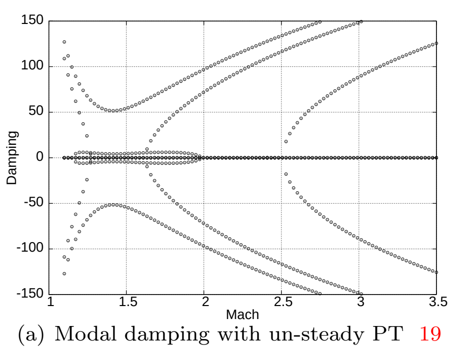

(a) Modal damping with un-steady PT 19

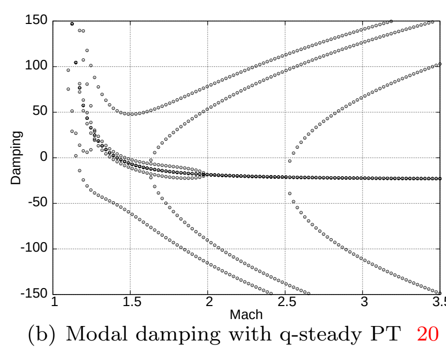

(b) Modal damping with q-steady PT 20

Figure 7. Modal damping trend with $\rho = 0.86$ $[Kg/m^3]$

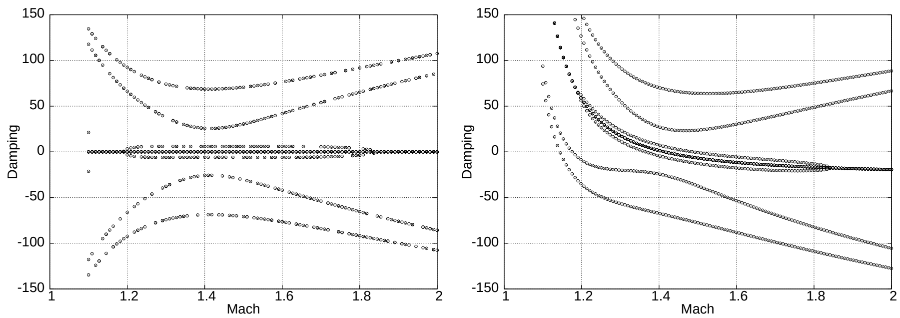

(a) Modal damping with un-steady PT 19 (b) Modal damping with q-steady PT 20

Figure 8. Modal damping trend focused in the range $1.1 < M < 2$ with $\rho = 0.9$ $[Kg/m^3]$

Next two figures, represent the 5th aeroelastic mode, instable, obtained by each aerodynamic theory in correspondence of $M = 1.35$ and $\rho = 1$ $[Kg/m^3]$.

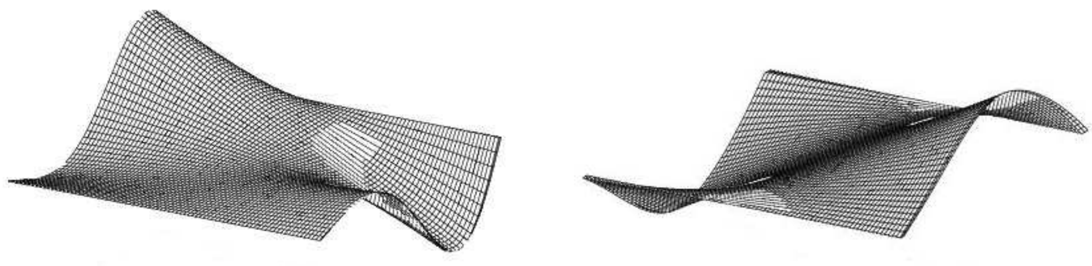

(a) Fifth modal shape with un-steady PT 19 (b) Fifth modal shape with q-steady PT 20

Figure 9. Fifth modal shape at $M = 1.35$, unstable

D. Panel made by composite materials

A common solution in the VTI panels design, consists of build multilayered composite structure. In particular, recent solutions include a sandwich structure, with a lightweight core and two multilayered skins. These skin may be of different composite materials, depending on the operative conditions. In this work have been used carbon composite skins, composed by two layer for each of them, with the following fiber orientation: $[45;-45]_s$. Two different materials have been used, their properties are respectively for the skin: orthotropic material with $\rho = 1560$ $[Kg/m^3]$, $E_{11} = 8.5 \times 10^{10}$ $[Pa]$, $E_{22} = 1.5 \times 10^9$ $[Pa]$, $E_{33} = 1.5 \times 10^9$ $[Pa]$, $G_{12} = 1.6 \times 10^9$, $G_{13} = 1.6 \times 10^9$ $[Pa]$, $G_{23} = 1.8 \times 10^9$, $\nu_{12} = 0.3$, $\nu_{13} = 0.3$, $\nu_{23} = 0.45$, $h = 0.0001$ $[m]$; while for the core: isotropic material with: $\rho = 80$ $[Kg/m^3]$, $E_{11} = E_{22} = E_{33} = 5.4 \times 10^7$ $[Pa]$, $G_{12} = G_{13} = G_{23} = 2.3 \times 10^7$ $[Pa]$, $\nu_{12} = \nu_{13} = \nu_{23} = 0.17391305$, $h = 0.008$ $[m]$. The panel has a length of 0.5 $[m]$, and is width of 1 $[m]$. Total thickness is 0.0084 $[m]$. It is simply supported on the major sides. The structural models used for this purpose were the Equivalent Single Layer and the Layer Wise, both of second and third order. Layer Wise model allows to better appreciate the strain field of a sandwich structure, due to its formulation; this advantage is felt especially in multilayered and sandwich elements. In order to demonstrate the importance of using a more advanced structural model for multilayered components, it is proposed a comparison between the previous models, consist of the research of flutter critical condition. For this purpose, have been chosen to fix the flow density to $\rho = 0.9$ Kg/m^3. The following table, shows the critical mach and the corresponding frequency, using the quasi-steady Piston Theory formulation.

Table 3. **Critical Mach and flutter frequencies with $\rho = 0.9\ Kg/m^3$**

$Model$	$Critical\ Mach$	$Flutter\ frequency$ $[Hz]$	$NDOF$
$LW2$	4.401	224.569	2178
$LW3$	2.966	203.252	3993
$ESL2$	5.245	228.864	726
$ESL3$	4.760	220.735	1089

Models based on ESL formulation, resulted unsuitable for multilayered panel. In fact, comparing this results with those previously obtained from single-layer isotropic panel, the gap among different structural model is very considerable. Consequently, becomes mandatory in order to correctly predicts the critical conditions, to adopt a LW structural model.

E. Application of previous structural theories on a typical VTI panel configurations

The VTI panel geometry chosen consist of a semi-circle with radius $R = 1.49\ m$ and length along flow direction of $L = 1.5\ m$. The panel is pinched in 10 points, divided in 5 constraints equally spaced on the leading edge, and many other on the trailing edge. This configuration is well-integrated with the pyrotechnical panel releasing device, hence represents one of the most appreciate solutions for this cases. Until today, a wide range of constraint systems have been tested with the aim of both ensure stability during the early flight phase and to provides a reliable panel release system. Despite this, panel flutter involves an extremely large amount of variables, that should be considered for a good design, however the problem becomes more and more complex and may be required experimental tests. The material properties of the VTI panel here used, are the same of the previous section. Past tests on curved panels, shown an increase of stiffness due to its geometry, in particular Dowell[24] in 1970, demonstrates how curvature improves the aeroelastic behavior of the panel. This effects are constituted by an enlargement of the stability region. The following results have been obtained with ESL structural model of third and fourth order, using quasi-steady Piston Theory formulation. Flow density has been fixed to $0.363\ Kg/m^3$.

Table 4. **Critical Mach and flutter frequencies for a VTI panel with $\rho = 0.363\ Kg/m^3$**

$Model$	$Critical\ Mach$	$Flutter\ frequency$ $[Hz]$	$NDOF$
$ESL3$	4.782	103.201	1521
$ESL4$	4.663	102.670	2028

Next images represent the sixth and the first modal shape obtained using ESL 4 model. The low number of grid elements are a limit for the graphic rendering, nevertheless it is still possible to appreciate local deflection in the central section of the panel. In particular, the sixth mode is unstable. Considerable deformation is visible along panel sides. This phenomenon was already seen in past tests, and could be reduced improving the panel stiffness along the sides, for example adding more constraints or using lightweight stiffening brackets.[25]

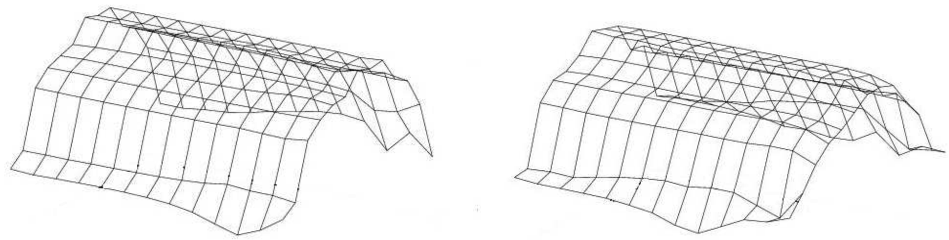

(a) Sixth modal shape

(b) First modal shape

Figure 10. Modal shapes in correspondence of $M = 4.663$, with $\rho = 0.363\ Kg/m^3$, model ESL4, quasi-steady Piston Theory

IV. Conclusions

As already shown by Vedeneev researches, the un-steady formulation of the Piston Theory, doesn't lend itself to correctly predicts eigenfrequencies and any transition from stability to instability of each mode, in particular in very low supersonic regime, where non-linear effects become relevant. However, compared to the quasi-steady formulation, has shown many relevant differences: stable modes, may have both negative or null damping, instead instable modes have only positive dumping. Numerically, this is related to the presence of the imaginary term, but doesn't affects the accuracy of the un-steady theory above $M = 1.5$. Dumping factor trend below this threshold, highlight the different behavior of certain modes, that may appear always stable, while with the q-s formulation tend to instability for progressively lower mach numbers. As stated by Vedeneev, it isn't possible to correctly predicts single mode flutter below this limit, using the Piston Theory; more complex aerodynamic theories are requested. However this new formulation, focuses the attention on behaviors before unseen with the q-s PT, suggesting more exhaustive researches, both numerical and experimental. Passing to analyze which information different structural models have provided, it was found that results regarding simple panels, in particular single-layer isotropic panels, are in good agree wether you're using a $1D$ Beam model that the Shell model. Results obtained by ESL or LW formulation, are in line with those collected by means of EDTN models. Lower order models, such us FSDT or Eulero-Bernoulli were not considered due to their inadequacy to represent complex modal shapes. Nevertheless, introducing multilayered panels, becomes essential the use of LW models, as shown by the results regarding the research of the panel critical condition. Compared with the ESL, results obtained through LW show an advance in the occurrence of flutter instability. Consequently is considered a good choice, to use more detailed models when composites and multilayered structures are used. Last test done, concerning a typical VTI panel configuration, permitted to observe different modal shapes in correspondence of the critical Mach. However this tests, not only neglect a large amount of variables of the real problem, such us internal acoustics effects and thermal-fluidynamic, complex to implement in the aeroelastic model, but using a less accurate models such as ESL on a sandwich panel, they aren't able to describe correctly each eigenfrequency trend and the correspondent dumping factor for a wide range of mach numbers. The correlation between the dumping factor and the aerodynamic theory, suggests also a careful interpretation of the data obtained, raising the use of LW models for the structural part and to specifically analyze ambiguous trends of the dumping factor.

References

[1]Lall, T. R., "Interstage adapter panel flutter on Atlas-Centaur AC-2, AC-3 and AC-4 vehicles," *Nasa technical memorandum TM X-1179*, 1965.

[2]Dowell, E. H., "Panel Flutter," *Nasa Space Vehicle Design Criteria SP-8004*, 1964.

[3]Carrera, E. and Zappino, E., "Development of a FE model suitable for Piston Theory (Supersonic Flow)analysis of VTI-panels with real BCs, 4/6 points pinched case. Calculation of critical Mach number." *Journal of Fluid and Structures*, 2011.

[4]Ashley, H. and Zartarian, G., "Piston theory - a new aerodynamic tool for the aeroelastician," *Composites Structures*, 1956, pp. 1109–1118.

[5]Cinefra, M Carrera, E., "Refined Shell elements," .

[6]Reddy, J. N., *Mechanics of laminated composite plates and shells. Theory and Analysis*, CRC Press, 2nd ed., 2004.

[7]Carrera, E., Giunta, G., and Petrolo, M., *Beam Structures: Classical and Advanced Theories*, John Wiley & Sons, 2011, DOI: 10.1002/9781119978565.

[8]Carrera, E. and Giunta, G., "Refined beam theories based on a unified formulation," *International Journal of Applied Mechanics*, Vol. 2, No. 1, 2010, pp. 117–143, DOI: 10.1142/S1758825110000500.

[9]Carrera, E. and Petrolo, M., "Refined beam elements with only displacement variables and plate/shell capabilities," *Meccanica*, Vol. 47, 2012, pp. 537–556.

[10]Carrera, E. Brischetto, S. and Nali, P., *Plates and Shells for Smart Structures: Classical and Advanced Theories for Modeling and Analysis*, John Wiley & Sons, 2011.

[11]Carrera, E., Giunta, G., Nali, P., and Petrolo, M., "Refined beam elements with arbitrary cross-section geometries," *Computers and Structures*, Vol. 88, No. 5–6, 2010, pp. 283–293, DOI: 10.1016/j.compstruc.2009.11.002.

[12]Carrera, E. and Petrolo, M., "A beam formulation with shell capabilities," *Proceedings of 51st AIAA/ASME/ASCE/AHS/ASC Structures, Structural Dynamics, and Materials Conference*, Orlando, Florida, USA, April 2010.

[13]Bolotin, V., "Nonconservative problems of the Theory of Elastic Stability," *Pergamon Press, Oxford*, 1963.

[14]Garric, I.E. Rubinow, S., "Flutter and oscillating Air-Force Calculation for an Airfoil in a two-dimensional supersonic flow," *NACA report No. 846*, 1946.

[15]Miles, J., "The potential theory of Unsteady supersonic flow," *Cambridge University Press, Cambridge*, 1959.

[16]Nelson, H. C. and Cunnigham, H. J., "Theoretical investigation of flutter of two-dimensional flat panels with one surface exposed to supersonic potential flow," *NACA report No. 1280.*, 1956.

[17]Dowell, E. H., "Nonlinear oscillation of fluttering plane," *AIAA Journal*, Vol. 4, 1966, pp. 1267–1275.

[18]Dowell, E. H., "Nonlinear oscillation of fluttering plane II," *AIAA Journal*, Vol. 5, 1967, pp. 1856–1862.

[19]Dowell, E. H., "Generalized aerodynamic forces on a flexible plate undergoing transient motion in a shear flow with an application to panel flutter," *AIAA Journal*, Vol. 9, 1971, pp. 834–841.

[20]Gordiner, R. E. and Visbal, M. R., "Development of a three-dimensional viscous aeroelastic solver for nonlinear panel flutter," *Journal of Fluids and Structures*, Vol. 16, 2002, pp. 497–527.

[21]Hashimoto, A Aoyama, T. and Nakamura, Y., "Effects of turbulent boundary layer on panel flutter," *AIAA Journal*, Vol. 47, 2009, pp. 2785–2791.

[22]Vedeneev, V. V., Guvernyuk, S. V., Zubkov, A. F., and Kolotnikov, M. E., "Experimental observation of single mode panel flutter in supersonic gas flow," *Journal of Fluid and Structures*, Vol. 26, 2010, pp. 764–779.

[23]Vedeneev, V. V., "Panel flutter at low supersonic speed," *Journal of Fluid and Structures*, Vol. 29, 2012, pp. 79–96.

[24]Dowell, E. H., "Panel flutter: A review of the aeroelastic stability of plates and shell," *AIAA Journal*, Vol. 8, 1970, pp. 385–399.

[25]Carrera, E. and Zappino, E., "VTI real panel guidelines and results summary reports," 2012.